# INSTITUTE FOR FUSION STUDIES

DE-FG05-80ET-53088-690 IFSR #690

**Numerical Simulation of Bump-on-Tail Instability with Source and Sink**

H.L. BERK, B.N. BREIZMAN, and M. PEKKER
Institute for Fusion Studies
The University of Texas at Austin
Austin, Texas 78712

**February 1995**

# THE UNIVERSITY OF TEXAS


# AUSTIN

# Numerical simulation of bump-on-tail instability with source and sink

H.L. Berk, B.N. Breizman,[a] and M. Pekker
*Institute for Fusion Studies, The University of Texas at Austin*
*Austin, Texas 78712*

A numerical procedure has been developed for the self-consistent simulation of the nonlinear interaction of energetic particles with discrete collective modes in the presence of a particle source and dissipation. A bump-on-tail instability model is chosen for these simulations. The model presents a kinetic nonlinear treatment of the wave-particle interaction within a Hamiltonian formalism. A mapping technique has been used in this model in order to assess the long time behavior of the system. Depending on the parameter range, the model shows either a steady-state mode saturation or quasiperiodic nonlinear bursts of the wave energy. We demonstrate that the mode saturation level as well as the burst parameters scale with the drive in accordance with the analytical predictions. We also quantify the threshold for the resonance overlap condition and particle global diffusion in the phase space. For the pulsating regime, we show that when $\gamma_L > 0.16\Delta\Omega$, where $\gamma_L$ is the linear growth rate for the unperturbed system and $\Delta\Omega$ is the frequency separation of neighboring resonances, overlap occurs together with an amplification of the free energy release compared to what is expected with the saturation of nonoverlapping modes. The effect of particle losses on the wave excitation is included in our model, which illustrates in a qualitative way the bursting collective losses of fast ions/alpha particles due to Alfvén instabilities.

PACS 52.35.Qz, 52.35.Ra, 52.40.Mj



[a] Also at Budker Institute of Nuclear Physics, Novosibirsk 630090, Russia

# I. INTRODUCTION

In this paper we will present results of the simulations of the bump-on-tail instability with a weak source and sink. We have posed this problem as a paradigm for the important problem in controlled fusion, that of the unstable excitation of Alfvén waves in a tokamak by resonant energetic alpha particles. The source of alpha particles is the controlled fusion reaction produced by the background plasma and the sink is the collisional transport processes that slow down or scatter the energetic particles. The mathematical techniques that are needed to address this applied problem can be demonstrated in the much simpler bump-on-tail problem, which is explained in this paper. In a later work we will present results for the Alfvén-alpha particle problem.

The essential physics that we address here is common to a wide variety of problems. We assume:

1. Instability is weak with the following properties: (a) the growth rate $\gamma$ is much less than the wave frequency; (b) instability is caused by the conversion free energy of energetic particles to wave energy; (c) the bulk of the particles (excluding the resonant particles) interact "adiabatically" with the wave.

2. There are sources and sinks present that allows a steady state solution for the particle distribution in the absence of waves.

3. Unstable modes have a discrete spectrum. Depending on system parameters they either behave as isolated modes that saturate due to local wave trapping or they overlap nonlinearly and produce global diffusion.

These features have been discussed previously from an analytical point of view in several papers.[1–4] One purpose of this paper is to confirm with numerical simulations the predictions

that arise from the analytic arguments. In addition we wish to build a numerical tool that can be used to study the effects of instability for the class of problems we are concerned with. In the text we describe the special numerical methods we have developed.

In our numerical method we use the fact that the wave structure of a discrete number of waves is known. One can show, using Hamiltonian techniques, that there is a standard form for the interaction between a resonant particle and a wave, even for complicated geometry. The response of the background plasma can be expressed in terms of the electromagnetic field, so that the Lagrangian for the waves includes both the contribution from the electromagnetic field and the background particles. In this paper we use this general structure for our relatively simple system.

We choose to obtain, using a Hamiltonian technique, similar to the one used in Ref. 5, a symplectic map to increment the amplitudes and phases of the waves and the coordinates of the particles for a time step $\tau$ such that $\omega^{-1} \ll \tau \ll \gamma^{-1}, \omega_b^{-1}$, where $\gamma$ is the growth rate of a wave, $\omega_b$ is the trapping frequency of a resonant particle with the wave and $\omega$ is the mode frequency. With this large time step, the code is very fast and efficient. The symplectic structure ensures an accurate evaluation of orbits that may or may not undergo stochastic diffusion from the waves. The symplectic structure of the map also implies that the resonant particles have incompressible motion in phase space. The property of incompressibility can be used as a "Lagrangian" grid to describe relaxation due to classical transport. With the relaxation mechanism included, one can observe a pulsating response of the system due to the reformation of the unstable state as opposed to a final relaxed state that would occur in an initial value problem without sources and sinks.

In the bump-on-tail problem described here the transport will be due to particle annihilation and a particle source. More general transport algorithms can be developed. A similar method has been used to evolve distribution functions in the "$\delta f$" algorithm.[6,7]

An important question we address is when mode overlap is likely to occur given the equilibrium parameters of the linear theory with a growth rate $\gamma_L$ and the frequency separation of neighboring resonances $\Delta\Omega$. For the bump-on-tail problem in the pulsating regime, we show that when $\gamma_L/\Delta\Omega > 0.16$ (a relatively small number) mode overlap occurs. Then if there are several linear modes present, global diffusion of the resonant particle occurs over the region where unstable modes are located.

In Sec. II, we derive a reduced Lagrangian for the nonlinear interaction of waves with energetic particles that resonate with the waves. Technically, our goal is to minimize the number of dynamical variables in the Lagrangian, subject to physics restrictions. We will assume that the number of energetic particles is relatively small, so that these particles have no effect on the spatial structure of the waves. It is also essential that wave amplitudes remain small, so that the finite amplitude waves retain the structure of the linear eigenmodes. The appropriate dynamical variables for these waves are their amplitudes and phases, which change as the waves interact with resonant particles. In Secs. III–V, we present our numerical results on the simulation of: the dynamics of single mode saturation, resonance overlap between two neighboring modes, and the collective bursts in particles losses, respectively. Section VI contains a brief summary and a comparison of our model with the phenomenological predator-prey model.[8] Two appendices describe: A) the connection between the macroparticle weight used in our simulations and the particle distribution function, and B) the derivation of the generating function for the mapping algorithm.

## II. LAGRANGIAN FORMALISM FOR WAVE-PARTICLE INTERACTION

We present the derivation of the simplified Lagrangian for energetic electrons interacting with plasma waves in a cold plasma, but we present it in a way that allows generalization to more complicated problems.

Our starting point will be the exact Lagrangian for charged particles in an electromagnetic field

$$L = \sum_{\text{plasma particles}} \int \left[ \frac{mv^2}{2} + \frac{e}{c}(\mathbf{A}\cdot\mathbf{v}) - e\phi \right] \delta(\mathbf{r}-\mathbf{r}_i) dV + \frac{1}{8\pi}\int (E^2 - B^2) dV$$

$$+ \sum_{\text{energetic electrons}} \int \left[ \frac{mv^2}{2} + \frac{e}{c}(\mathbf{A}\cdot\mathbf{v}) - e\phi \right] \delta(\mathbf{r}-\mathbf{r}_i) dV, \qquad (1)$$

where $\mathbf{r}_i$ is the particle coordinate and $\mathbf{v} = \dot{\mathbf{r}}_i$ is the particle velocity. Since plasma particles adiabatically respond to the fields, their contribution to the Lagrangian can be expressed in terms of the field variables. With this simplification, the first two terms in Eq. (1) give a Lagrangian for the waves $L_w$:

$$L_w = \sum_{\text{plasma particles}} \int \left[ \frac{mv^2}{2} + \frac{e}{c}(\mathbf{A}\cdot\mathbf{v}) - e\phi \right] \delta(\mathbf{r}-\mathbf{r}_i) dV + \frac{1}{8\pi}\int (E^2 - B^2) dV$$

$$- \sum_{\text{plasma particles}} \int \left[ \frac{mv_0^2}{2} + \frac{e}{c}(\mathbf{A}_0\cdot\mathbf{v}_0) - e\phi_0 \right] \delta(\mathbf{r}-\mathbf{r}_{i0}) dV - \frac{1}{8\pi}\int (E_0^2 - B_0^2) dV, \qquad (2)$$

where we have subtracted out a constant in the Lagrangian so that $L_w = 0$ when perturbations vanish and the subscript "0" refers to the unperturbed quantities. This expression will depend only on field variables, as shown below.

It should be noted that, to lowest order, the wave Lagrangian $L_w$ is quadratic with respect to the wave amplitudes since the linear terms vanish due to the fact that the equilibrium state satisfies a minimum action principle.

In the present work, we restrict ourselves to one-dimensional electrostatic electron perturbations with plasma ions forming an immobile uniform background. For these perturbations, it is most convenient to choose to represent the electric field $E$ as a time derivative of $A_x(x;t)$, with $A_x(x;t)$ the only nonzero component of the vector potential, namely

$$E = -\frac{1}{c}\dot{A}_x. \qquad (3)$$

Gauge invariance has allowed us to impose a restriction that the scalar potential $\phi$ vanishes. In a cold spatially uniform plasma all the unperturbed quantities in Eq. (2) are equal to zero

and also there is no perturbed magnetic field in our problem (i.e., $B = 0$). As in our gauge there are no linear terms, the quadratic nature of the response is manifest (with other choices of gauge, more careful manipulation is required to demonstrate the quadratic response). We then obtain,

$$L_w = \sum_{\text{plasma particles}} \left( \frac{m{v_x}^2}{2} + \frac{e}{c} A_x(\mathbf{r}_i, t) v_x \right) + \frac{1}{8\pi} \int E_x^2 dV. \tag{4}$$

We now use the equation of motion for plasma electrons obtained from variation of $L_w$ with respect to $x_i$ (the other terms in the Lagrangian are independent of the cold plasma variables), and find

$$\dot{v}_x = -\frac{e}{mc} \dot{A}_x \tag{5}$$

With one integration, we use the relation

$$v_x = -\frac{e}{mc} A_x \tag{6}$$

to express $v_x$ in terms of $A_x$ in the Lagrangian. Then $L_w$ becomes

$$L_w = \frac{1}{8\pi c^2} \int \left( \dot{A}_x^2 - \omega_p^2 A_x^2 \right) dV, \tag{7}$$

where $\omega_p$ is the electron plasma frequency. Note that we use

$$\frac{4\pi e^2}{m} \sum_{\text{plasma particles}} A_x^2(\mathbf{r}_i) = \int \omega_p^2 A_x^2 dV$$

because we ignore density modulations in the sum which are higher order in $A_x$ and we ignore spatial fluctuations arising from the discreteness of the homogeneous ensemble of particles.

Next, we represent $A_x$ as a superposition of linear plasma modes

$$A_x = \sum_{\text{modes}} A_k \exp(-i\alpha_k - i\omega_p t + ikx) + \text{c.c.}$$

where real mode amplitudes $A_k(t)$ and phases $\alpha_k(t)$ are slowly varying functions of time. We then neglect rapidly oscillating terms in the Lagrangian as their contribution nearly vanishes

on integrating over space. Hence, the variation of such terms produces a negligible response to the coefficients of the varied quantities. We then obtain

$$L_w = \frac{V\omega_p}{2\pi c^2} \sum_{\text{modes}} \dot{\alpha}_k {A_k}^2, \tag{8}$$

where $V$ is the system volume. We assume this volume to be sufficiently large so that no physical quantity would depend on it. By taking the extremum of this Lagrangian to form the Euler equations, the equations of motion for free waves are found to be

$$\begin{aligned} \dot{A}_k &= 0 \\ \dot{\alpha}_k &= 0. \end{aligned} \tag{9}$$

Although we have derived Eq. (8) for a particular case of plasma waves, this equation has in fact a general feature that the structure of the Lagrangian for other waves with a slowly varying amplitude and phase is exactly the same as will be further demonstrated in subsequent work. The cogent point is that in weak turbulence theory, the lowest order wave Lagrangian is always proportional to $\dot{\alpha}_k {A_k}^2$ with $\alpha_k$ and $A_k$ generalized phase and amplitude factors.

We now turn to the energetic particle Lagrangian that can be written in the form

$$L_{\text{part}} = \frac{m\dot{x}^2}{2} + \frac{e}{c} \sum_{\text{modes}} \dot{x} A_k \exp(-i\alpha_k - i\omega t + ikx) + \text{ c.c.} \tag{10}$$

where $x$ is the particle coordinate. At this point, it is appropriate to make use of the fact that, for the particle to interact with a mode, its velocity $\dot{x}$ must be close enough to the mode phase velocity $\omega_p/k$. This allows us to replace $\dot{x}$ with $\omega_p/k$ in the interaction term, i.e., under the summation sign in Eq. (10). Next, we combine Eqs. (10) and (8) to obtain the complete Lagrangian for particles and waves.

$$\begin{aligned} L = &\frac{V\omega_p}{2\pi c^2} \sum_{\text{modes}} \dot{\alpha}_k {A_k}^2 + \sum_{\text{energetic electrons}} \frac{m\dot{x}^2}{2} \\ &+ \frac{e\omega_p}{c} \sum_{\text{modes}} \sum_{\text{energetic electrons}} \frac{1}{k} A_k \exp(-i\alpha_k - i\omega t + ikx) + \text{ c.c. .} \end{aligned} \tag{11}$$

We then define new variables for the waves

$$P = \left(\frac{V\omega_p}{\pi mc^2}\right)^{1/2} A_k \cos\alpha_k, \qquad Q = \left(\frac{V\omega_p}{\pi mc^2}\right)^{1/2} A_k \sin\alpha_k, \tag{12}$$

so that the Lagrangian becomes

$$\frac{L}{m} = \sum_{\text{modes}} P\dot{Q} + \sum_{\text{macroparticles}} q\frac{\dot{x}^2}{2}$$
$$+ \sum_{\text{modes}} \sum_{\text{macroparticles}} qS_k \left[P\cos(kx-\omega t) + Q\sin(kx-\omega t)\right], \tag{13}$$

where

$$S_k = \frac{e}{k}\left(\frac{4\pi\omega_p}{mV}\right)^{1/2}$$

In addition to having changed variables, we have also changed the sum over real particles to the sum over macroparticles, which has introduced the macroparticle weight factor $q$ into Eq. (13). The macroparticles represent the elements of the phase space that experience an area preserving motion along the Hamiltonian orbits. It follows from the Liouville theorem that, without a particle source and collisions, the weight of each macroparticle is a conserved quantity. It is also convenient to alter the term $\dot{x}^2/2$ in the Lagrangian to $v\dot{x} - v^2/2$, with velocity $v$ a new momentum-like independent variable. In this case, the self-consistent set of equations for wave-macroparticle dynamics has the form

$$\dot{Q} = -\sum_{\text{macroparticles}} qS_k \cos(kx-\omega t), \tag{14}$$

$$\dot{P} = \sum_{\text{macroparticles}} qS_k \sin(kx-\omega t), \tag{15}$$

$$\dot{x} = v, \tag{16}$$

$$\dot{v} = \sum_{\text{modes}} kS_k \left[-P\sin(kx-\omega t) + Q\cos(kx-\omega t)\right]. \tag{17}$$

It is easy to verify that the alteration of the Lagrangian reproduces identical equations of motion.

A more general set of equations, which we actually solve in this paper, has three additional factors, not included in Eqs. (14)–(17). First, we add a background dissipation of the plasma waves at a given damping rate $\gamma_d$ that is not associated with resonant particles. This damping modifies Eqs. (14) and (15) to

$$\dot{Q} = - \sum_{\text{macroparticles}} qS_k \cos(kx - \omega t) - \gamma_d Q, \tag{18}$$

$$\dot{P} = \sum_{\text{macroparticles}} qS_k \sin(kx - \omega t) - \gamma_d P. \tag{19}$$

Second, we introduce a source, $S(v)$, of energetic particles, and, third, we assume that these particles undergo an annihilation process at a rate $\nu_r$, which tends to balance the source and establish a steady state particle distribution. Formally, we describe the source and relaxation effects with the following time evolution equation for the macroparticle weight:

$$\dot{q} = S(v) - \nu_r q. \tag{20}$$

Equations (16) and (17) remain unchanged, so that the closed set of equations to be solved now consists of Eqs. (16)–(20). In Appendix A we show that our formulation is equivalent to solving for a distribution function, $f$, that satisfies the kinetic equation

$$\frac{\partial f}{\partial t} + [H, f] = S(v) - \nu_r f, \tag{21}$$

The essential point in achieving this equation is that the particle motion is incompressible in a $v, x$ phase space.

Our modified set of equations does not have a Hamiltonian structure. However, the non-Hamiltonian terms in these equations are relatively small since typically the source and relaxation processes are sufficiently weak, so that they do not cause a significant change in the particle distribution function on the time scale of the order of the inverse instability growth rate. Also, the wave damping from the background plasma is often small compared to the linear growth rate. Clearly, the shortest time scale that characterizes our problem

is determined by the linear instability growth rate with the system dynamics being essentially Hamiltonian over this time scale. To eliminate numerical diffusion in propagating the Hamiltonian system, we construct our numerical scheme as an area-preserving map to which we then add non-Hamiltonian corrections due to $\gamma_d$, $S$, and $\nu_r$. We have found that an appropriate generating function for the map is

$$\Phi = \sum_{\text{modes}} \hat{P}Q + \sum_{\text{macroparticles}} q\left(\hat{v}x + \tau\frac{\hat{v}^2}{2}\right)$$

$$- \sum_{\text{modes}} \sum_{\text{macroparticles}} qS_k\tau\left[\hat{P}\cos(kx-\omega t) + Q\sin(kx-\omega t)\right] G[(k\hat{v}-\omega)\tau], \qquad (22)$$

where $\tau$ is the time step, the hat-sign marks the time advanced quantities, and $G(x) = 1$ if $x \ll 1$ and $G(x)$ vanishes if $x \gg 1$. In our simulations, we use $G(x) = \sin x/x$. The derivation of this generating function is given in Appendix B. The time step $\tau$ is chosen so that $\gamma\tau \ll 1$. If $(k\hat{v}-\omega)\tau \ll 1$, the correct particle dynamics is obtained. Note that the contribution of particles with $(k\hat{v}-\omega)\tau > 1$, though not correct, is not essential as their interaction is small since they are not resonant. The whole scheme can now be written as

$$\hat{x} = \frac{1}{q}\frac{\partial\Phi}{\partial\hat{v}}, \qquad v = \frac{1}{q}\frac{\partial\Phi}{\partial x}, \qquad (23)$$

$$\hat{Q} = \frac{\partial\Phi}{\partial\hat{P}} - Q\gamma_d\tau, \qquad P = \frac{\partial\Phi}{\partial Q} + \hat{P}\gamma_d\tau, \qquad (24)$$

$$\hat{q} = q + S(v)\tau - q\nu_r\tau. \qquad (25)$$

An important advantage of this map-based algorithm is that it allows the energetic particles to be rapidly processed on the time-scale of the inverse instability growth rate; this is much more efficient than following the particle dynamics on the inverse mode frequency time scale.

## III. SINGLE MODE SIMULATIONS

The purpose of these simulations is to illustrate and verify two different regimes of mode saturation predicted by analytical theory: steady state saturation that establishes when the

particle relaxation rate $\nu_r$ exceeds the background damping rate $\gamma_d$, and a bursting scenario that occurs in the opposite limiting case. The physics essence of these regimes has been described in Refs. 1 and 2.

We first discuss the steady state saturation shown in Fig. 1. In this simulation the system starts with no energetic particles but with the source turned on. As particles are injected and stored, the resonant particles excite a plasma wave, whose wave energy is shown as a function of time in Fig. 1a. We see that the wave energy approaches a steady state level. The distribution function is shown in Fig. 1b and one should note the nearly flattened distribution function at the resonant velocity, which here is marked as $v_{\rm res}$.

The calculated mode amplitude in the steady-state regime agrees well with the following analytical formula derived in Ref. 9:

$$\omega_b = 1.9\gamma_L \frac{\nu_r}{\gamma_d}, \tag{26}$$

where $\gamma_L$ is the contribution to the linear growth rate from the equilibrium distribution of energetic particles without waves. Here, $\omega_b$ is the nonlinear bounce frequency of resonant particles which is given by

$$\omega_b = \left(\frac{ekE}{m}\right)^{1/2} \tag{27}$$

with $E$ the electric field amplitude of the mode, and $k$ the wavenumber. This agreement is illustrated by Fig. 2 that shows the dependence of the particle bounce frequency at saturation on the background damping rate.

The difference between the theoretical curve and the simulation results can be attributed to the fact that, at a low damping rate, the plateau around the resonant velocity $v_{\rm res}$ (see Fig. 3) extends beyond the interval where the unperturbed distribution function is of constant slope.

The second simulation in this section is for a larger damping rate, which causes the wave energy to pulsate in time, as shown in Fig. 4a. In accordance with the analytical estimates,

the value of $\omega_b$ at a pulse maximum is of the order of $\gamma_L$ and the typical time interval between the pulses is of the order of $\nu_r^{-1}$. When we examine the shape of the distribution for this case, we see that distribution function near $v_{res}$, has an appreciable slope just prior to the pulse onset (see Fig. 4b), and the local distribution is flattened when the wave energy achieves its maximum level (see Fig. 4c). Our simulations show that the bursts are not exactly periodic in time, and also that their amplitudes vary. The physics reason behind these statistical variations is that, between the bursts, the system evolves into a metastable state that may "crash" if triggered by a fluctuation. More analytic work is needed to quantify the probability of these fluctuations and its relation to the intrinsic discreteness of both physical and numerical systems. Even though the individual bursts fluctuate, their average properties, that are determined by the energy balance condition, appear to be quite stable and predictable. We have checked this conclusion by making several longer runs (up to $t = 2500\gamma_L^{-1}$), the results of which are summarized in Fig. 5. This figure shows that the average burst energy defined by the formula

$$\overline{W} = \frac{1}{N}\sum_{i=1}^{N} W_i, \tag{28}$$

where $W_i$ is the peak energy of the $i$-th burst and $N$ is the number of bursts scales as the fourth power of the linear growth rate, in agreement with the expectation that $\omega_b \sim \gamma_L - \gamma_d$. We have quantitatively determined that

$$\overline{\omega}_b = 1.4(\gamma_L - \gamma_d) \tag{29}$$

with $\overline{\omega}_b$ the average value of $\omega_b$. The statistical variations in $\omega_b$ are relatively small, namely, $\Delta\omega_b/\omega_b < 0.05$. We have also benchmarked our code against earlier simulations of the initial value bump-on-tail problem without a source[10] and found the two to be in precise agreement. In particular, both simulations show that the ratio $\omega_b/\gamma_L$ at mode saturation is 3.2.

# IV. RESONANCE OVERLAP AND STOCHASTIC DIFFUSION

Even with more than one mode present in the system, the steady-state or pulsating nonlinear scenario may apply to each mode separately if the neighboring resonances do not overlap. Then the saturated waves would cause the distribution function to flatten locally near each resonance. However, when the resonances overlap at the saturation level, stochastic motion of particles arises, which allows individual particles to diffuse in phase space over many resonances so that the particle distribution can flatten over a large region of velocity space. It has been noted that much more particle kinetic energy transforms to wave energy during global flattening than arises when overlap does not occur.[1,4] We can observe this trend in simulations with two unstable modes. In the resonance region of the two modes, particle mixing tends to flatten the distribution function while no significant change in the distribution function has been observed outside the resonance region. The results of the two mode simulations are presented in Figs. 6 and 7. Similar to the previous single mode runs, the system starts with no energetic particles but with the source turned on. As the injected particles accumulate, the slope of their distribution function builds up gradually and so does the linear instability growth rate. At an intermediate stage when the system is already linearly unstable but the modes saturate at a relatively low level in accordance with the instantaneous estimate

$$\omega_b \sim \gamma_L \tag{30}$$

the snapshot of the particle distribution function (see Fig. 7a) shows two separate local plateaus, one near each resonance. These plateaus broaden and eventually merge into the global plateau shown in Fig. 7c. Note that the corresponding bursts in the wave energy are now an order of magnitude greater than those shown in Fig. 4 for a single mode, although the particle source, the relaxation rate and the background damping have exactly the same values as in the single-mode run. The burst enhancement is caused by the larger free energy

that becomes available when modes overlap. The plateau then broadens giving rise to a free energy release that is proportional to the cube of the plateau width.

The resonance overlap condition can generally be presented in the form

$$\omega_b > Ck\delta v = C\Delta\Omega, \tag{31}$$

where $\delta v$ is the difference in phase velocities between the neighboring modes and $C$ is a numerical factor. Our two-mode simulations show that the factor $C$, which determines the threshold of global diffusion, is close to 0.22. This estimate holds for both pulsating and steady state regimes. With Eq. (29) for the pulsating regime ($\gamma_d$ is now assumed negligible) we find that resonance overlap occurs when $\gamma_L > 0.16k\delta v$.

# V. SIMULATIONS OF BURSTS IN PARTICLE LOSSES

In this section, we consider a model problem that suggests a plausible mechanism for the bursts of energetic particle losses that have been observed in fast ion beam experiments in a tokamak. In order to relate the results of this subsection to the fast ion-Alfvén wave problem in a tokamak, one has to take into account that the velocity space diffusion in our model should be interpreted as a spatial diffusion in the fast ion-Alfvén wave problem.

To simulate the losses within our model, we introduce a particle collector in velocity space at $v < v_c$, where $v_c$ is the collector edge position. The particle source is assumed to be zero for $v < v_c$, and the particle absorption rate in the collector, $\nu_c$, is taken to be twenty times greater than $\nu_r$. With such a source, the particles can only reach the collector if their distribution broadens due to the interaction with unstable modes. Otherwise, every particle would be absorbed where it was born, i.e. at $v > v_c$.

In these simulations we use four modes with the phase velocities $v_1$, $v_2$, $v_3$, and $v_4$, respectively, all of which are above the collector edge. Shown in Fig. 8 is the time evolution of the mode energy, which exhibits bursts that occur simultaneously in all four modes.

Synchronized with these bursts, are the bursts in the particle flux at the collector, which are shown in Fig. 9. The snapshots of the particle distribution function presented in Fig. 10 demonstrate that the losses at the collector are indeed coherent with the broadening of the particle distribution at the moments of the wave energy bursts.

# VI. CONCLUSION

In this work we described the simulation of the bump-on-tail instability with sources and sinks. We have chosen the bump-on-tail instability as this is the simplest problem in kinetic theory that describes the response of a continually driven system, where the steady-state without perturbations has a weak instability driven by resonant particles.

This problem indicates that, depending on conditions, the system can produce steady oscillations, or pulsating oscillations. Further the nature of the oscillations can be due to saturation by local flattening of the distribution or global flattening. In the former case, wave trapping of resonant particles by single modes releases a modest amount of wave energy, and there is no global diffusion of these resonant particles. In the latter case, the mode amplitudes cause global overlap of modes and the collapse of the entire distribution over the phase space region that overlaps with waves. The result is a much larger release of wave energy density. As discussed in Ref. 3, without mode overlap, the wave energy density scales as $N$, where $N$ is the number of modes. At the point that mode overlap occurs, the wave energy release will scale as $N^3$. Our simulations qualitatively reproduce this enhancement.

The other interesting feature of our model is the observed bifurcation that arises in the character of the particle diffusion. When the resonances do not overlap, the instability saturates by flattening the particle distribution locally in phase space and particles only mix in the resonant region of a single mode. However, when the linear growth rate becomes too large, neighboring unstable modes can be excited and cause mode overlap. In these simulations of the bump-on-tail problem overlap occurs in the pulsating regime when $\gamma_L/$

$\Delta\Omega > 0.16$. This is a rather low number and its absolute value may be problem specific. Nonetheless the result is indicative that on-set of global diffusion when a discrete set of modes are unstable, occurs at substantially lower values of $\gamma_L$ than is expected from the dimensional estimate $\gamma_L/\Delta\Omega \sim 1$, although the scaling is preserved. Then when resonance overlap arises, the resulting amplification of the wave energy produces global diffusion over the entire area of phase space covered by the excited modes and particle resonances. If the area of enhanced diffusion includes the boundaries of the system a rapid loss of particles may occur.

The quasiperiodic pulsations of the wave energy, which occur within our model, have some similarity with those of the predator-prey model, a common model in recent investigations.[8,11] The predator-prey model captures the feature that the growing mode saps the free energy of the wave, and then the sources have to resurrect the unstable structure. However, the predator-prey model has a basic weakness that the period of pulsations is rather arbitrarily determined by the choice of initial conditions. Even a steady response can be obtained with an appropriate initial condition. In our kinetic model, the choice of a pulsating or steady state response does not depend on initial conditions. Rather the nature of the response depends on the physical quantities that define equilibrium and linear stability of the system; these include the characteristics of the source, sink and background damping and the wavenumbers of unstable modes. It is also important that, in contrast with the predator prey model, our model is based on the systematic derivation of the nonlinear dynamics from the fundamental equations of motion.

## Acknowledgments

This work was supported by the U.S. Department of Energy Contract No. DE-FG05-80ET-53088.

# APPENDIX A: CONNECTION BETWEEN THE MACROPARTICLE WEIGHT AND THE PARTICLE DISTRIBUTION FUNCTION

Let us consider the distribution function,

$$f = \sum_{\text{particles}} q_i(t)\delta(x - x_i(t))\delta(v - v_i(t)) \tag{A1}$$

where $q(t)$, $x_i(t)$ and $v_i(t)$ satisfy the equations,

$$\begin{aligned} \dot{q} &= S(v) - \nu_r\, q \\ \dot{v}_i &= -\frac{\partial H}{\partial x_i} \\ \dot{x}_i &= \frac{\partial H}{\partial v_i}, \end{aligned} \tag{A2}$$

where $H$ is the Hamiltonian per unit mass. By taking the time derivative of Eq. (A1) we obtain

$$\frac{\partial f}{\partial t} = \sum_{\text{particles}} \begin{bmatrix} \dot{q}_i(t)\delta(x - x_i(t))\delta(v - v_i(t)) \\ -\dot{x}_i(t)\,\frac{\partial}{\partial x}\,\delta(x - x_i(t))\delta(v - v_i(t)) \\ -\dot{v}_i(t)\,\frac{\partial}{\partial v}\,\delta(x - x_i(t))\delta(v - v_i(t)) \end{bmatrix} \tag{A3}$$

Then using (A2) gives

$$\frac{\partial f}{\partial t} + [H, f] = \sum_{\text{particles}} \left(S(v) - \nu_r\, q_i(t)\right)\delta(x - x_i(t))\delta(v - v_i(t)). \tag{A4}$$

Now we choose the distribution $\sum_i \delta(x - x_i(t))\delta(v - v_i(t))$ so that it is initially statistically homogeneous in phase space over the region where $x_i(t)$ and $v_i(t)$ will evolve to. For an incompressible motion in phase space, $\sum_i \delta(x - x_i(t))\delta(v - v_i(t))$ remains statistically spatially homogeneous and therefore constant in time. Then

$$\sum_{\text{particles}} S(v)\delta(x - x_i(t))\delta(v - v_i(t)) = S(v).$$

The term with $\nu_r$ in (A4) is by definition $\nu_r f$. Thus, we have demonstrated that Eq. (A1) satisfies

$$\frac{\partial f}{\partial t} + [H, f] = S(v) - \nu_r f.$$

## APPENDIX B: DERIVATION OF THE GENERATING FUNCTION

We use the fact that the function that generates the transformation to time-advanced quantities in the Hamiltonian motion is $-S$, where $S$ is the action written as a function of the old coordinates $q_i$ and the time-advanced quantity $\widehat{q}_i$; we mark all time-advanced quantities with the hat-sign.[12] The transformation is implicitly determined by the relations

$$\widehat{p}_i = \frac{\partial S(q_i; \widehat{q}_i)}{\partial \widehat{q}_i}, \qquad p_i = -\frac{\partial S(q_i; \widehat{q}_i)}{\partial q_i}, \tag{B1}$$

from which $\widehat{q}_i$ and $\widehat{p}_i$ can be found as a function of $q_i$ and $p_i$. Since, in our problem, $p_i$ is constant in the unperturbed motion whereas $q_i$ changes with time, it is more convenient to use $\widehat{p}_i$ and $q_i$ as the independent variables of the generating function. Then the appropriate generating function changes from $-S$ to

$$\Phi = -S + \sum \widehat{q}_i \widehat{p}_i, \tag{B2}$$

and the new coordinates and old momenta are

$$\widehat{q}_i = \frac{\partial \Phi}{\partial \widehat{p}_i}, \qquad p_i = \frac{\partial \Phi}{\partial q_i}. \tag{B3}$$

Now using the

$$\widehat{q}_i - q_i = \int_t^{t+\tau} \dot{q}_i(t) dt,$$

where $\tau$ is the time step, we can rewrite Eq. (B2) in the form

$$\Phi(\widehat{p}_i; q_i) = \sum q_i \widehat{p}_i - \int_t^{t+\tau} L dt + \sum \widehat{p}_i \int_t^{t+\tau} \dot{q}_i(t) dt, \tag{B4}$$

where the first term on the right-hand side describes the identity transformation. Using Eq. (13) for the Lagrangian and noting that the particle velocity does not change significantly

if $\tau \ll \gamma^{-1}, \omega_b^{-1}$, we then calculate the last two terms approximately by integrating over the unperturbed motion. which gives

$$\Phi = \sum_{\text{modes}} \hat{P}Q + \sum_{\text{macroparticles}} q\left(\hat{v}x + \tau\frac{\hat{v}^2}{2}\right)$$

$$- \sum_{\text{modes}} \sum_{\text{macroparticles}} qS_k\tau\left[\hat{P}\cos(kx-\omega t) + Q\sin(kx-\omega t)\right]\frac{\sin[(k\hat{v}-\omega)\tau]}{(k\hat{v}-\omega)\tau}$$

$$- \sum_{\text{modes}} \sum_{\text{macroparticles}} qS_k\left[-\hat{P}\sin(kx-\omega t) + Q\cos(kx-\omega t)\right]\frac{1-\cos[(k\hat{v}-\omega)\tau]}{k\hat{v}-\omega}. \quad \text{(B5)}$$

The last term in this expression can be dropped since, for the resonant particles with $kv - \omega \approx \gamma$, this term is quadratic in $\tau$ and therefore much smaller than the first interaction terms in $\Phi$. In addition, the form-factor $\sin x/x$ in the first interaction term can be altered to improve numerical filtering. Namely, the key features of the model should not change if we replace this factor with a function $G(x)$ that equals 1 when $x$ is small, decays rapidly for $x \gg 1$, and has the same norm as $\sin x/x$ (in order to properly capture the linear growth rate). This generalization is then a convenient way of cutting off insignificant contributions from nonresonant particles.

## References


1. H.L. Berk, B.N. Breizman, and H. Ye, Phys. Rev. Lett. **68**, 3563 (1992).

2. B.N. Breizman, H.L. Berk, and H. Ye, Phys. Fluids B **5**, 3217 (1993).

3. H.L. Berk and B.N. Breizman, Scenarios for the Nonlinear Evolution of Beam Driven Instability with a Weak Source, in Advances in Plasma Physics, Thomas H. Stix Symposium, AIP Conf. Proc. 314, edited by N. Fisch (American Institute of Physics, New York, 1994), p. 140.

4. H.L. Berk, B.N. Breizman, and M. Pekker, "Basic Principles Approach for Studying Nonlinear Alfvén Wave-Alpha Particle Dynamics," in *Physics of High Energy Particles in Toroidal Systems,* AIP Conf. Proc. 311, edited by T. Tajima and M. Okamoto, (American Institute of Physics, New York, 1994), p. 18.

5. J.R. Cary and I. Doxas, J. Comp. Phys. **107**, 98 (1993).

6. M. Kotschenreuther, Bull. Am. Phys. Soc. **33**, 2107 (1988).

7. R.E. Denton and M. Kotschenreuther, $\delta f$ Algorithm, IFS Report IFSR No. 629, November 1993.

8. W.W. Heidbrink, H.H. Duong, J. Manson, E. Wilfrid, C. Oberman, and E.J. Strait, Phys. Fluids B **5**, 2176 (1993).

9. H.L. Berk and B.N. Breizman, Phys. Fluids B **2**,2226 (1990).

10. B.D. Fried, C.S. Liu, R.W. Means, R.Z. Sagdeev, "Nonlinear evolution and saturation of an unstable electrostatic wave," Rep. PPG-93, University of California, Los Angeles (1971).

11. W.W. Heidbrink and J.R. Danielson, Phys. Plasmas **1**, 4120 (1994).

12. L.D. Landau and E.M. Lifshitz, Mechanics, Pergamon (1972).

# FIGURE CAPTIONS

FIG. 1. Steady-state nonlinear saturation of an isolated mode. (a) Time dependence of the mode energy. The wave energy density is normalized to $W_{\rm norm} = 0.5\,{\rm mnv}_{\rm res}^2(\gamma_L/\omega_p)^4$ where $\gamma_L$ is the contribution to the linear growth rate from the equilibrium distribution of energetic particles without waves, and $n$ is the plasma density. (b) Flattened particle distribution near the resonance: solid line — distribution at mode saturation, dashed line — unperturbed distribution. The normalized background damping and the relaxation rate in this run are $\gamma_d/\gamma_L = 0.031$ and $\nu_r/\gamma_L = 0.035$.

FIG. 2. Scaling law for the steady-state mode saturation at a given relaxation rate ($\nu_r/\gamma_L = 0.035$); solid line — analytical theory, data points — simulations.

FIG. 3. Particle distribution when mode is at steady-state saturation with $\nu_r/\gamma_L = 0.035$ and with very small background damping level ($\gamma_d = 0.018\gamma_L$).

FIG. 4. Nonlinear bursts of an isolated mode ($\gamma_d/\gamma_L = 0.082$, $\nu_r/\gamma_L = 0.0082$). (a) Time dependence of the mode energy. The wave energy density is normalized to $W_{\rm norm} = 0.5\,{\rm mnv}_{\rm res}^2(\gamma_L/\omega_p)^4$. (b) Particle distribution prior to burst ($\gamma_L t = 152$). (c) Particle distribution after the burst ($\gamma_L t = 175$).

FIG. 5. Comparison of the numerical and analytical results for the average burst energy as a function of the linear growth rate.

FIG. 6. Time evolution of the total wave energy for the nonlinear bursts of two overlapped modes with the phase velocities $v_1$ and $v_2$ such that $\frac{2\omega_p}{\gamma_L}\,\frac{v_1-v_2}{v_1+v_2} = 2.6$. The wave energy density is normalized to $W_{\rm norm} = 0.125\,{\rm mn}(v_1+v_2)^2(\gamma_L/\omega_p)^4$. The background damping and relaxation rate are same as in FIG. 4.

FIG. 7. Snapshots of the velocity distribution of resonant particles for the run shown in FIG. 6:

a) an early stage of the burst ($\gamma_L t = 73$) when the two modes have not yet overlapped (note the local plateaus near the resonances with each mode);

b) merging of the two resonant regions during the burst ($\gamma_L t = 85$);

c) globally flattened distribution immediately after the burst ($\gamma_L t = 98$).

FIG. 8. Time evolution of the wave energy in the simulation of particle losses caused by four bursting modes with equally spaced phase velocities $v_1$, $v_2$, $v_3$ and $v_4$ indicated in FIG. 10, such that $\frac{2\omega_p(v_1-v_2)}{\gamma_L(v_2+v_2)} = 2.4$. The normalized background damping and the relaxation rate in this run are $\gamma_d/\gamma_L = 0.18$ and $\nu_r/\gamma_L = 0.009$.

FIG. 9. Time dependence of the particle flux to the collector located at $v = v_c$ (see FIG. 10).

FIG. 10. Snapshots of the particle distribution function in the simulation of particle losses:

a) before the burst, when particles do not reach the collector;

b) during the burst when particles are being lost at the collector.

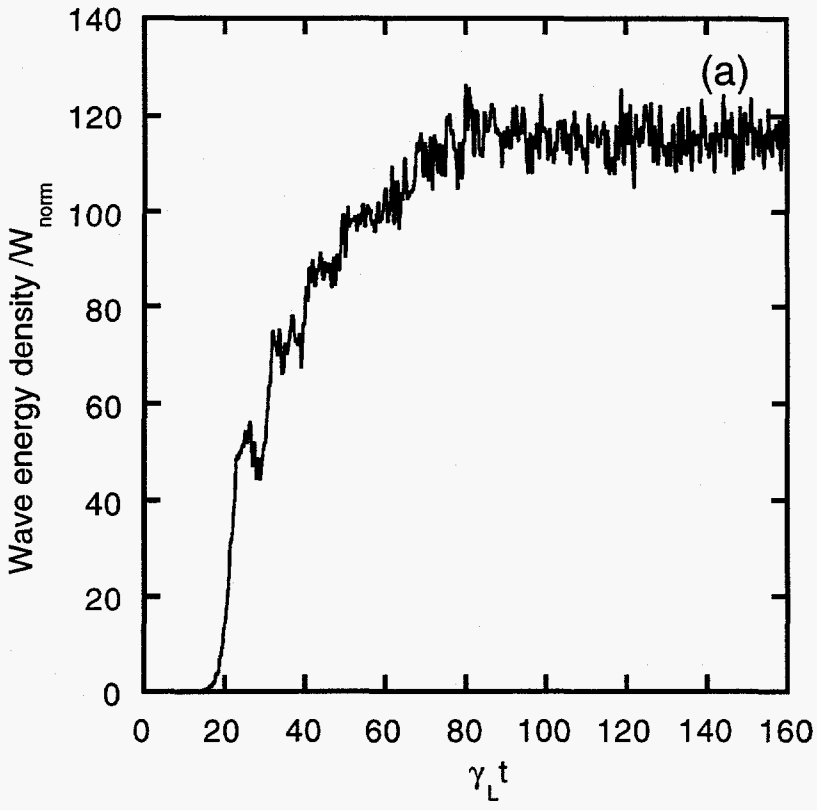
(a)
Wave energy density /W norm
140
120
100
80
60
40
20
0
0
20
40
60
80
100
120
140
160
γ L t

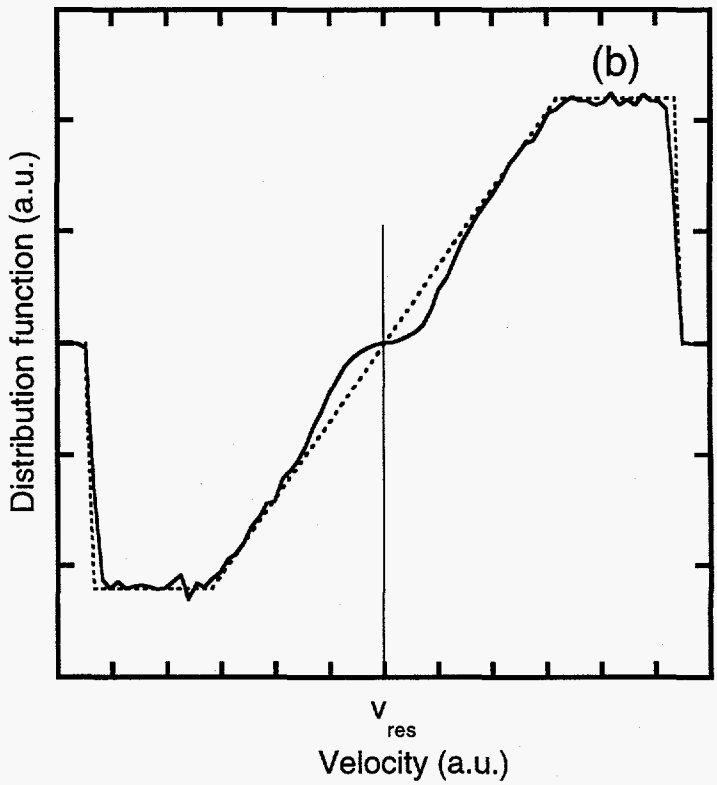
(b)
Distribution function (a.u.)
V res
Velocity (a.u.)

Figure 1

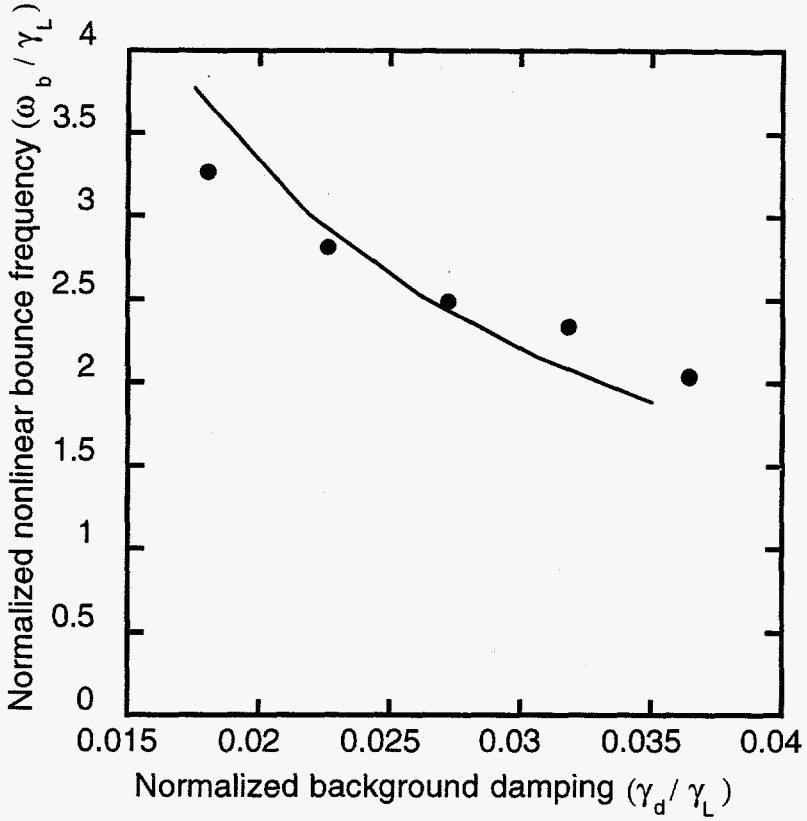


Figure 2

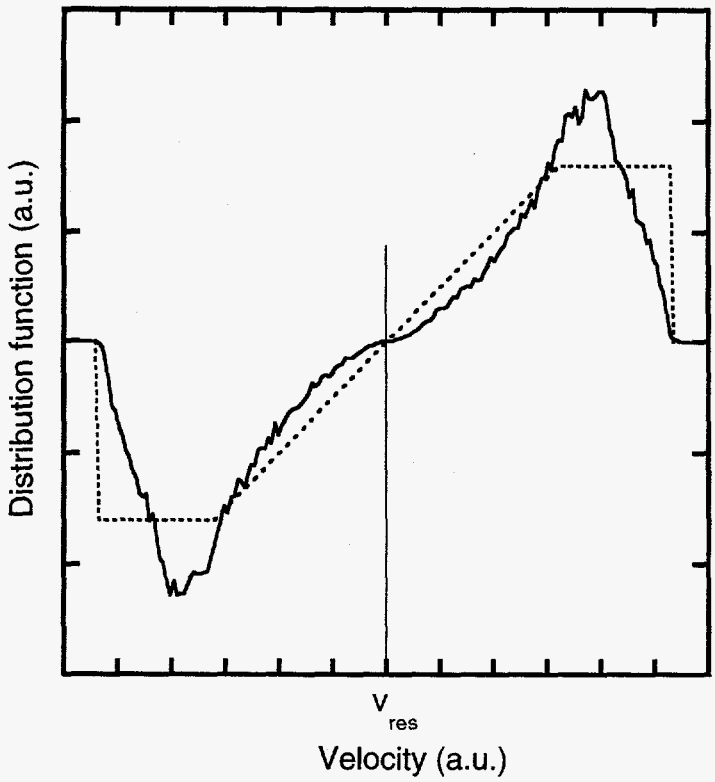


Figure 3

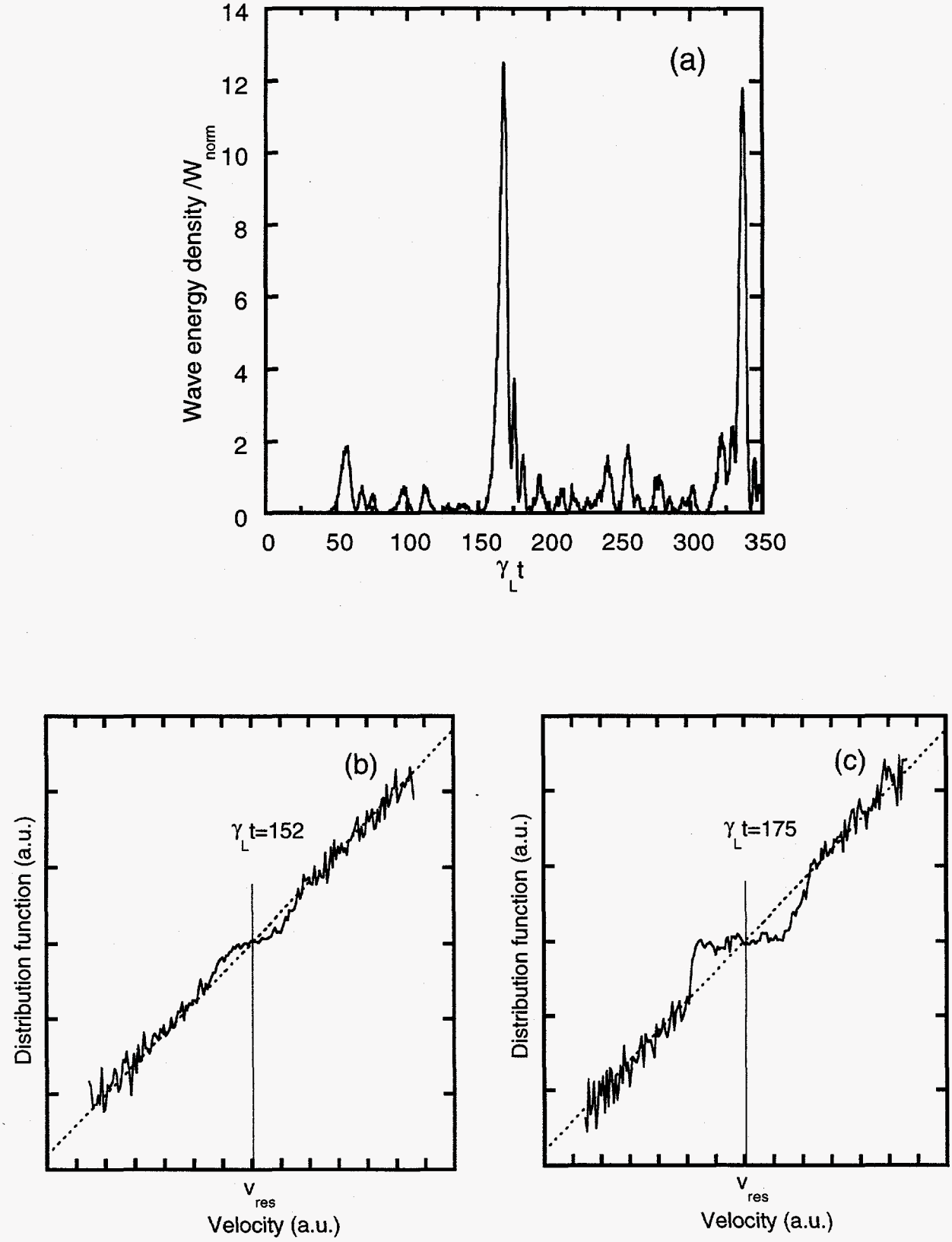
(a)
Wave energy density /W_norm
γ_L t
0
2
4
6
8
10
12
14
0
50
100
150
200
250
300
350
(b)
γ_L t=152
Distribution function (a.u.)
v_res
Velocity (a.u.)
(c)
γ_L t=175
Distribution function (a.u.)
v_res
Velocity (a.u.)

Figure 4

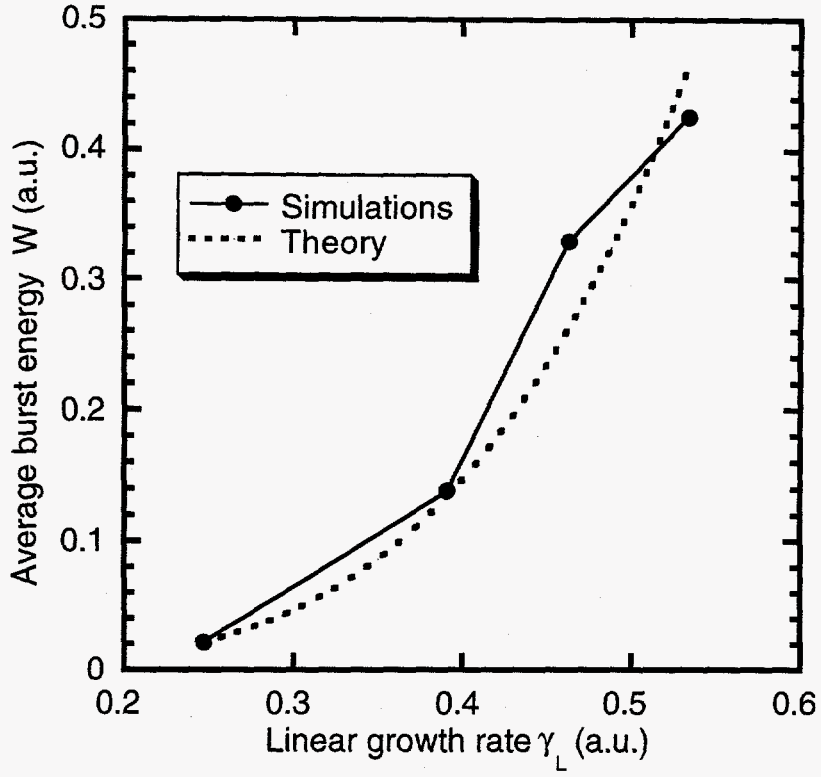


Figure 5

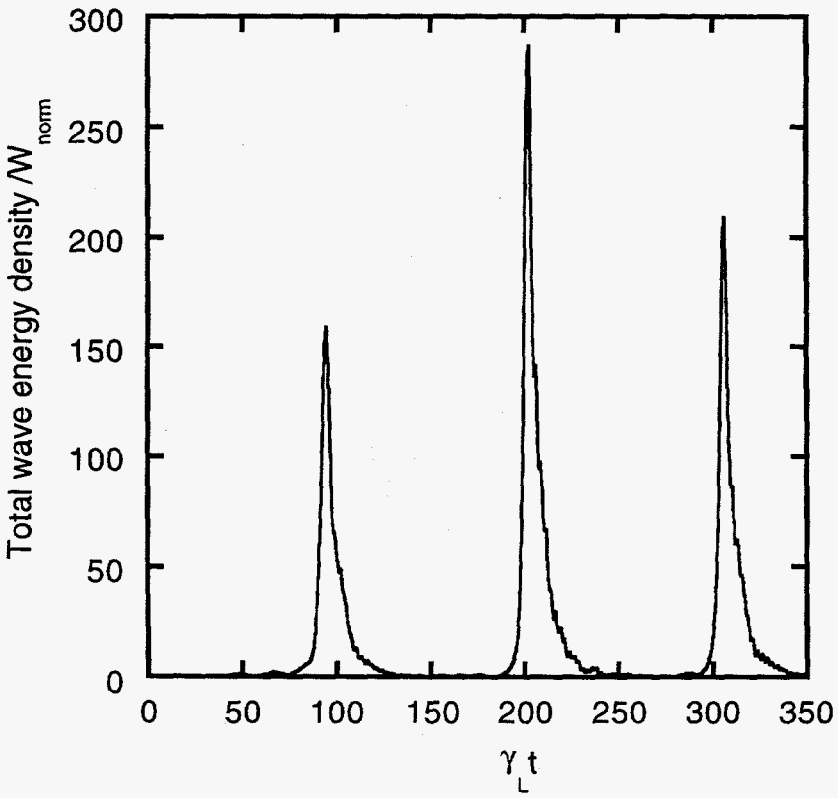


Figure 6

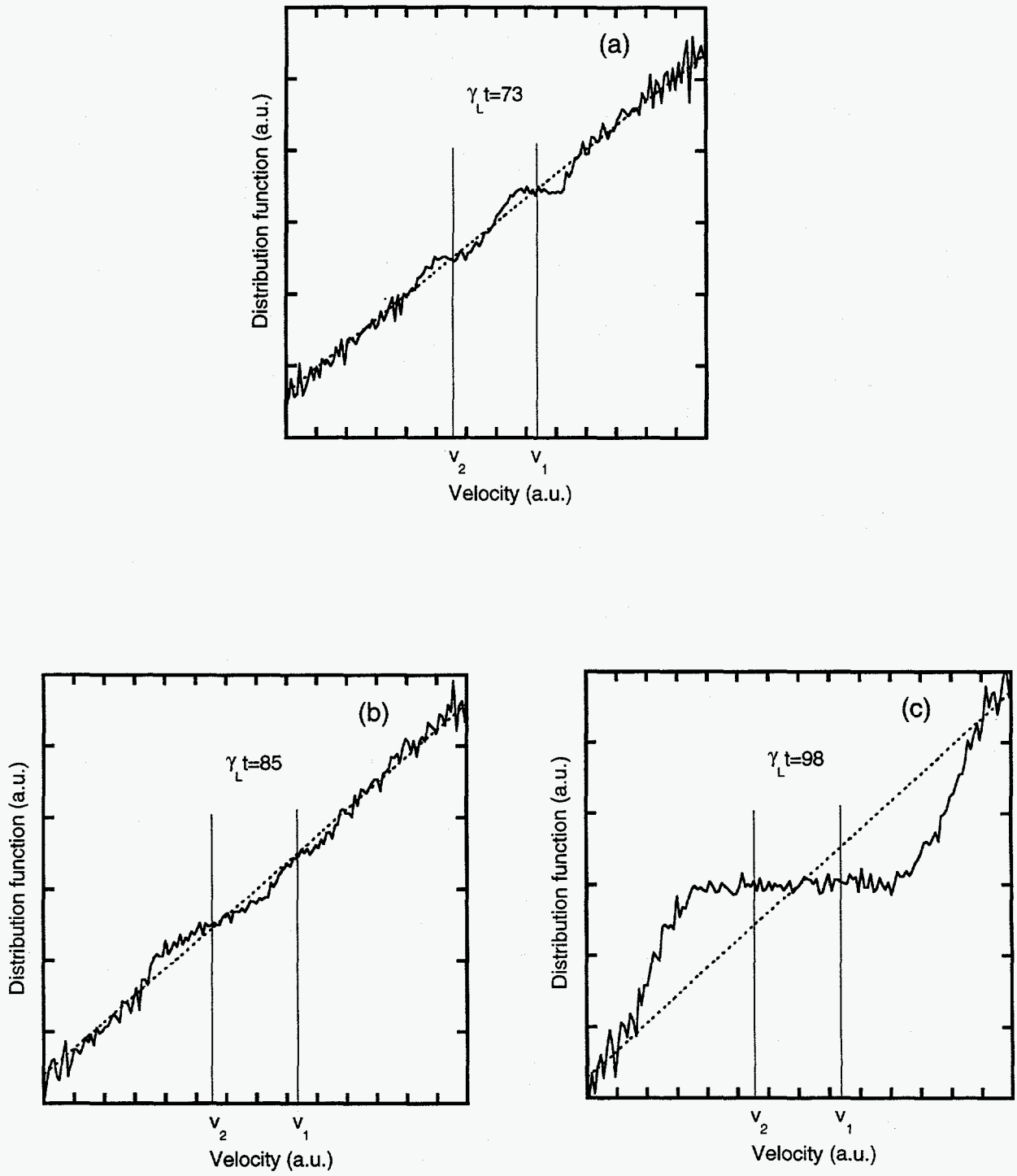
(a)
$\gamma_L$ t=73
Distribution function (a.u.)
$v_2$
$v_1$
Velocity (a.u.)
(b)
$\gamma_L$ t=85
Distribution function (a.u.)
$v_2$
$v_1$
Velocity (a.u.)
(c)
$\gamma_L$ t=98
Distribution function (a.u.)
$v_2$
$v_1$
Velocity (a.u.)

Figure 7

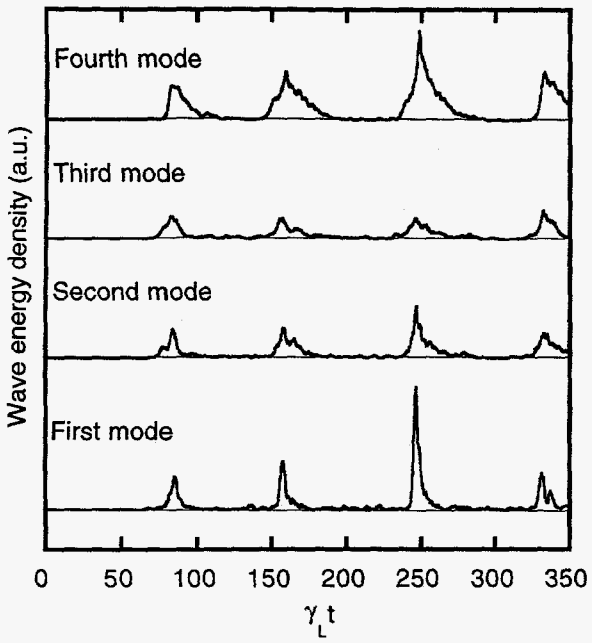


Figure 8

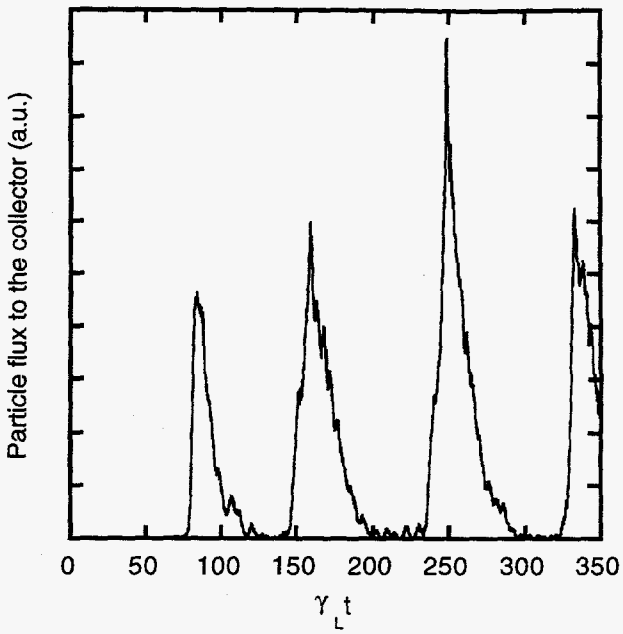


Figure 9

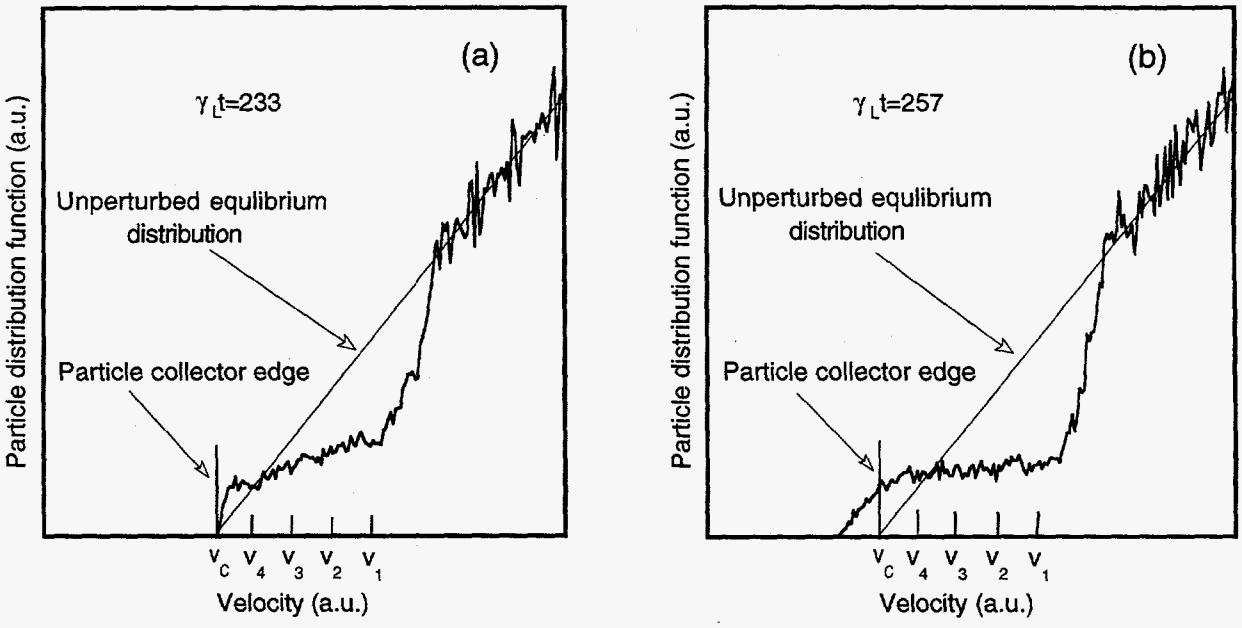


Figure 10